

Deformation Properties of Coarse-grained Materials from Cyclic and Monotonic Loading Triaxial Tests

by

Tsuneo UESAKA¹⁾, Hitoshi YOSHIDA²⁾ and Tomoya IWASHITA³⁾

ABSTRACT

Cyclic and monotonic loading triaxial tests on large-scale specimens of coarse-grained materials with differing relative densities were performed. The effects of bedding errors at the top and bottom ends of specimens were confirmed for coarse-grained materials. As the strain of a soil material is larger, its stiffness decays, which indicates strain-dependency of the stiffness, that is, non-linear properties of the material. The effects of the loading pattern on the testing, the grain shape of materials and the relative density of specimens on the strain-dependency of the Young's modulus of coarse-grained materials were evaluated. The strain-dependency of the Young's modulus of coarse-grained materials was compared with that of a fine sand.

Due to the bedding error, the Young's modulus of coarse-grained materials externally measured from the displacement of a cap was from 5% to 25% smaller than the locally measured ones for this test set. The Young's modulus from cyclic loading (CL) and that from monotonic loading (ML) tests almost agreed for a range of small axial strain less than 10^{-5} (0.001%). The strain-decay of Young's moduli of dense coarse-grained materials from the cyclic loading and monotonic loading tests differed from that of loose ones for a range of axial strain more than

about 5×10^{-5} (0.005%). The decay in the Young's modulus of the loose specimens with the increase in axial strain was smaller in the CL tests than in the ML tests. However, the decay in the Young's modulus of the dense specimens with the increase in axial strain was larger in the CL tests than in the ML tests. The strain-decay of Young's modulus of dense coarse-grained materials was different from that of sands.

Key Words : bedding error, coarse-grained materials, relative density, triaxial test, Young's modulus

1. INTRODUCTION

It is important to evaluate the non-linear properties of granular materials such as rockfill and gravel materials during strong quake motions for earthquake response analyses of rockfill dams and structures constructed on a gravel bed. The deformation properties of coarse-grained materials for a range of shear strains less than 0.1% become input material properties for response analyses, and have a

1) Director of Dam Department, Public Works Research Institute, Ministry of Construction
Tsukuba Science City, 305 Japan

2) Head of Fill Dam Division, ditto

3) Research Engineer, Fill Dam Division, ditto

significant effect on the dynamic response. As input values, the results by laboratory element tests or in-situ tests have been used. It is essential to improve the precision of the material stiffness measurement from laboratory tests. When axial deformation is measured from the external displacement, the axial strain may be over-estimated due to the bedding error between the ends of the specimen and the cap and pedestal of the triaxial cell. The bedding error occurs due to the looseness at the ends of the specimen and a poor fit between the specimen ends and the cap or the pedestal. The effect of the bedding error is larger for the tests on dense specimens of coarse-grained materials prepared in the laboratory than for tests on fine sands (Tatsuoka et al., 1992). This study confirms the effect of the bedding error for large-scale triaxial tests on coarse-grained materials having angular and round grain shapes. As the strain of a soil material increases, its stiffness decays, which indicates strain-dependency of the stiffness, that is, non-linear properties of the material. The strain-dependency of stiffness is affected by materials, specimen conditions, and testing methods, etc. We evaluate the effect of the loading pattern on the testing, the grain shape of materials and the relative density of specimens on the strain-dependency of Young's modulus of coarse-grained materials. We also compare the strain-dependency of Young's modulus of coarse-grained materials with that of a fine sand.

2. TESTED MATERIALS

The testing was performed with specimens compacted by two kinds (CRR and RBG) of coarse-grained materials. The material CRR consists of crushed gabbro rocks having angular shaped grains and the material RBG is riverbed andesite gravel having round shaped grains.

The physical properties of both materials are shown in Table 1.

3. EXPERIMENTAL METHOD

Triaxial tests on large specimens with a diameter of 300 mm and a height of 600 mm were performed. Photograph 1 shows the triaxial testing apparatus used in this study. A load cell installed inside the triaxial cell and combined with the cap of a specimen measured the axial load directly acting on the specimen without including piston friction. The local and external axial strains for a small range were measured. The local axial strains were measured by means of a local deformation transducer (LDT). The LDT is a thin strip of phosphor bronze on which a couple of strain gauges are attached at the central part of each side of the surface. The LDT strip is 500 mm long, 5 mm wide, and 1.2 mm thick, as shown in Photo. 2, and measured the deformation of the central part (approx. 47 cm) of the lateral surface of the specimen excluding the ends of the specimen, as shown in Photo. 3. The external axial strains (EXT) were measured from the displacement of a specimen cap to which a couple of targets were attached, using gap sensors installed on column standings fixed on the base of the triaxial cell, as shown in Photo. 4.

The specimens were prepared by compacting the materials with an electric vibrator in six layers. The specimens were set up in two kinds of relative density D_r of 50% (loose) and 85% (dense) for CRR, only 85% (dense) for RBG. The grain size distribution of the specimens was the same for both materials as shown in Figure 1. The top and bottom ends of the specimens were in contact with a porous stone disk fixed to the cap and pedestal. The

specimens were then saturated until a B-value of at least 0.95 was reached.

Consolidated drained triaxial tests were carried out with two loading patterns of cyclic loading (CL test) and monotonic compression loading (ML test). The cyclic loading triaxial tests (CL test) were performed by staged confining pressure testing in the each stage of which the confining pressure was gradually increased from lower pressure to higher pressure ($\sigma_c' = 0.1, 0.2, 0.4, 0.6$ MPa). Figure 2 shows a schematic figure of the process of the staged loading. At each loading stage with the constant lateral confining pressure, twelve cycles of symmetric sinusoidal cyclic axial stresses with a constant amplitude of deviator stress were applied at a loading frequency of 0.1 Hz on the specimen. As the stiffness of the specimen, the equivalent Young's modulus E_{eq} was obtained using the hysteresis loop of the tenth cyclic loading as shown in Figure 3 (a). The data of loads and displacements were filtered for more than 1.0 Hz and less than 0.0001 Hz. In the monotonic loading triaxial compression tests (ML test), a constant axial strain rate of 0.5 %/min was used. At the start of an operation, the loading piston and the triaxial chamber piston were separated to avoid the strain history acting on the specimen during the action of combining the pistons. At the time of the pistons contacting and load acting on a specimen just after the start of operation, the strain was defined as zero. The data of loads and displacements were fed at a sampling frequency of 200 Hz, and were filtered for more than 2.0 Hz. As the stiffness of the specimen, the secant Young's modulus E_{sec} was obtained for each sampling data as shown in Figure 3 (b).

4. RESULTS OF TESTS

(1) Effects of Bedding Error

The effects of the bedding error on strain measurements of gravel obtained from triaxial tests have been reported by several researchers (Tatsuoka et al., 1994, Hamano et al., 1995, and Tanaka et al., 1995). We compared the strain measurements from the LDT and the EXT for the tests on CRR and RBG. Figures 4 show the relationships between E_{eq} and the single amplitude axial strain $(\varepsilon_a)_{sa}$ from the CL tests on CRR and RBG, and Figures 5 show the relationships between the deviator stress $(\sigma_1 - \sigma_3)$ and the axial strain ε_a from the ML tests. The Young's modulus E_{eq} and the deviator stress $(\sigma_1 - \sigma_3)$ measured by the LDT are greater than those by the EXT for both the CL and ML tests. At an elastic range of $(\varepsilon_a)_{sa}$ of 10^{-5} or less, the differences of the stiffness are between 5% and 25% for the CL tests on both CRR and RBG.

(2) Comparison of Stiffness from Cyclic Loading and Monotonic Loading Tests

Figures 6 show the strain-decay curves of the Young's moduli E_{eq} and E_{sec} from the CL and ML tests plotted against ε_a for the ML tests and its single amplitude $(\varepsilon_a)_{sa}$ for the CL tests. For a range of small axial strain less than 10^{-5} , the Young's modulus from the CL test and that from the ML test almost agree for both CRR and RBG. The moduli at the initial small strain are constant, which shows that the deformation behaves elastically.

The rates of decay of the two Young's moduli E_{eq} and E_{sec} from the CL and ML tests respectively begin to differ for a range of axial strain more than about 5×10^{-5} . On the loose

specimen, whose relative density $Dr = 50\%$, the decay in the Young's modulus with increase in axial strain is smaller in the CL tests than in the ML tests. On the dense specimen, whose $Dr = 85\%$, the decay in the Young's modulus with increase in axial strain is, however, larger in the CL tests than in the ML tests. Figures 7 show hysteresis loops with single amplitude axial strain (ε_a) of about 2×10^{-4} from the CL tests on specimens with Dr of 50% and 85%. The cyclic strain of the loose specimen moves to the compressive side, so the hysteresis loop is not closed. The equivalent Young's modulus E_{eq} in Figure 6 (a), thus, is somewhat overestimated, but only by about 3%, and the decay of E_{eq} is unchanged from the tendency noted above.

Several researchers (Tatsuoka et al., 1994, and Hamano et al., 1994, etc.) have reported the comparisons between the locally measured stiffness of sand from the CL and the ML tests. Figures 8 show the strain decay curves of the Young's moduli, E_{eq} and E_{sec} , from the CL and the ML tests on loose ($Dr = 45\%$) and dense ($Dr = 70\%$) Toyoura sand which is Japanese fine sand (Tatsuoka et al., 1994). It can be seen from Figures 8 that, on sand also, the Young's modulus E_{eq} from the CL tests agrees well with the E_{sec} from the ML tests for a range of initial axial strain less than about 10^{-5} . The strain-dependency of Young's moduli E_{eq} and E_{sec} of sands, however, differs from that of coarse-grained materials shown in Figures 6. Regardless of the relative density of the sand specimens, the strain-dependency of Young's modulus of sand is smaller in the CL tests than in the ML tests for a range of more than about 5×10^{-5} .

Comparing Figures 6 and 8, the strain-dependency of Young's moduli E_{eq} and E_{sec} of

dense coarse-grained materials differs from that of dense sands. The strain-decay of Young's modulus of dense coarse-grained materials is larger in the CL tests than in the ML tests. On the other hand, the strain-decay of dense sands is smaller in the CL tests than in the ML tests. Dong et al. (1994) also reported similar results from the tests on various dense gravels whose Dr is greater than 80%, with the results for this set of tests on both the dense CRR and RBG specimens. Dong et al. explained these phenomena as follows. This difference between the deformation properties of sands in the CL tests and the ML tests is primarily due to the effect of cyclic strain hardening; i.e., the increase in the stiffness due to the change in the structure by drained cyclic loading itself. In the case of CL tests on dense gravels with constant lateral confining pressure, however, due to the high stiffness, as the cyclic strain amplitude becomes large, a reduction in the axial stress (thus the reduction in the mean stress) when loaded in triaxial extension becomes very large. This mechanism overwhelms the effect of cyclic strain hardening. The main reason why the strain-decay of Young's modulus of loose CRR specimens is similar to that of sands is that the effect of cyclic strain hardening overwhelms the effect of a reduction in the mean stress.

5. CONCLUSIONS

The test results of the cyclic and monotonic triaxial tests on loose and dense coarse-grained materials are summarized as follows.

- [1] Due to the bedding error, the Young's modulus externally measured from the displacement of a cap was 5% to 25% smaller than the locally measured modulus for this test set on coarse-grained materials.

- [2] The Young's modulus from cyclic loading and that from monotonic loading tests almost agreed for a range of initial small axial strain less than 10^{-5} .
- [3] The strain-decay of Young's moduli E_{eq} and E_{sec} of dense coarse-grained materials from cyclic loading and monotonic loading tests differed from that of loose coarse-grained materials. Comparing the results of coarse-grained materials with that of sands, the strain-decay of Young's modulus in cyclic loading and monotonic loading tests on loose coarse-grained materials was similar to those of the sands. The strain-decay of Young's modulus of dense coarse-grained materials, however, was different from that of sands.

REFERENCES

- Dong, J., Nakamura, K., Tatsuoka, F., and Kohata, Y. (1994): Deformation Properties of Gravels in Triaxial Compression Tests and Cyclic Triaxial Tests, Pre-failure Deformation of Geomaterials, Balkema, pp.17-23.
- Hamano, M., Toriihara, M., Hiram, K. (1994): Comparison Between Static and Dynamic Modulus of Deformation Using Small Strain Gauge, Proc. of the 29th Japan National Conference on Soil Mechanics and Foundation Engineering, The Japanese Society of Soil Mechanics and Foundation Engineering, pp.763-764.
- Hamano, M., Toriihara, M., Hiram, K. (1995): Dynamic Deformation Properties of Gravel Changed Grain Size Using Small Strain Gauge, Proc. of the 30th Japan National Conference on Soil Mechanics and Foundation Engineering, The Japanese Society of Soil Mechanics and Foundation Engineering, pp.957-958.
- Tanaka, Y., Kokusho, T., Okamoto, T., Kudo, K. (1995): Effect of Non-uniformity on Dynamic Deformation Properties of Gravel, Proc. of the 50th Annual Conference of The Japan Society of Civil Engineers, Vol. III, pp.460-461.
- Tatsuoka, F., and Shibuya, S. (1992): Deformation Characteristics of Soils and Rocks from Field and Laboratory Tests, Report of the Institute of Industrial Science, The University of Tokyo, Vol.37 No.1.
- Tatsuoka, F., Teachavorasinskun, S., Dong, J., Kohata, Y., and Sato, T. (1994): Importance of Measuring Local Strains in Cyclic Triaxial Tests on Granular Materials, Dynamic Geotechnical Testing, Vol. II, ASTM STP 1213, pp.288-302.

Table 1 Properties of the tested materials

		CRR	RBG
Density of soil particles	ρ_s (g/cm^3)	2.93	2.56
Water content	w (%)	0.54	1.03
Maximum void ratio	e_{\max}	0.569	0.432
Minimum void ratio	e_{\min}	0.142	0.167
Maximum grain size	D_{\max} (mm)	63.0	63.0
50% passing grain size	D_{50} (mm)	10.2	10.2
Uniformity coefficient	U_c	30	30
Grain shape		angular	round

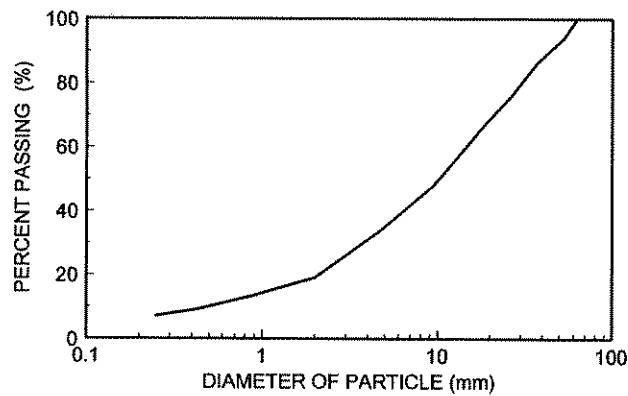


Figure 1 Grain size distribution curve of the tested materials

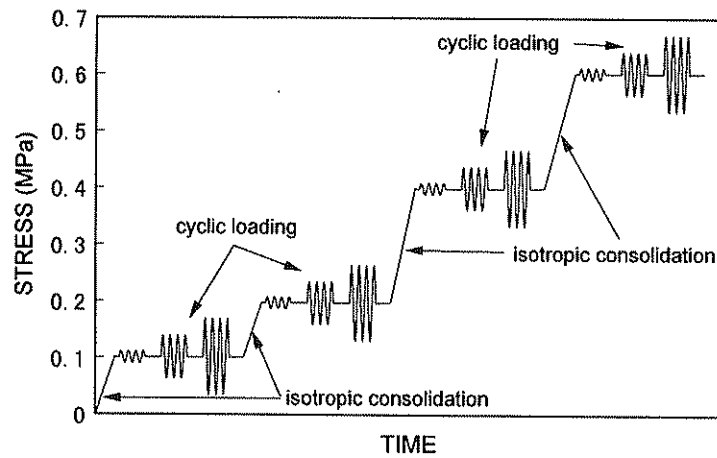
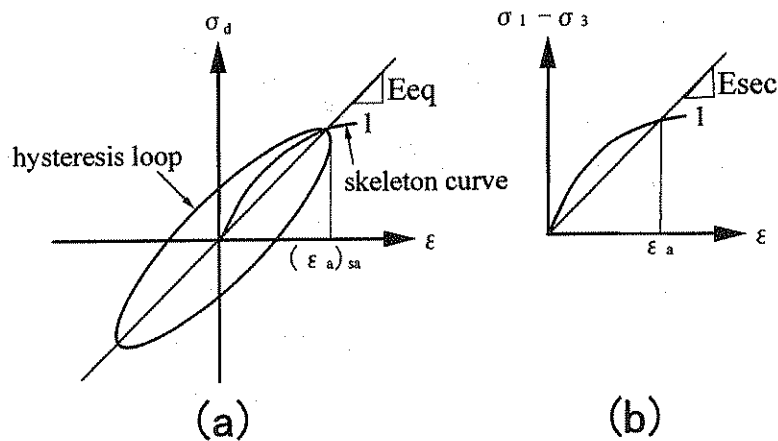
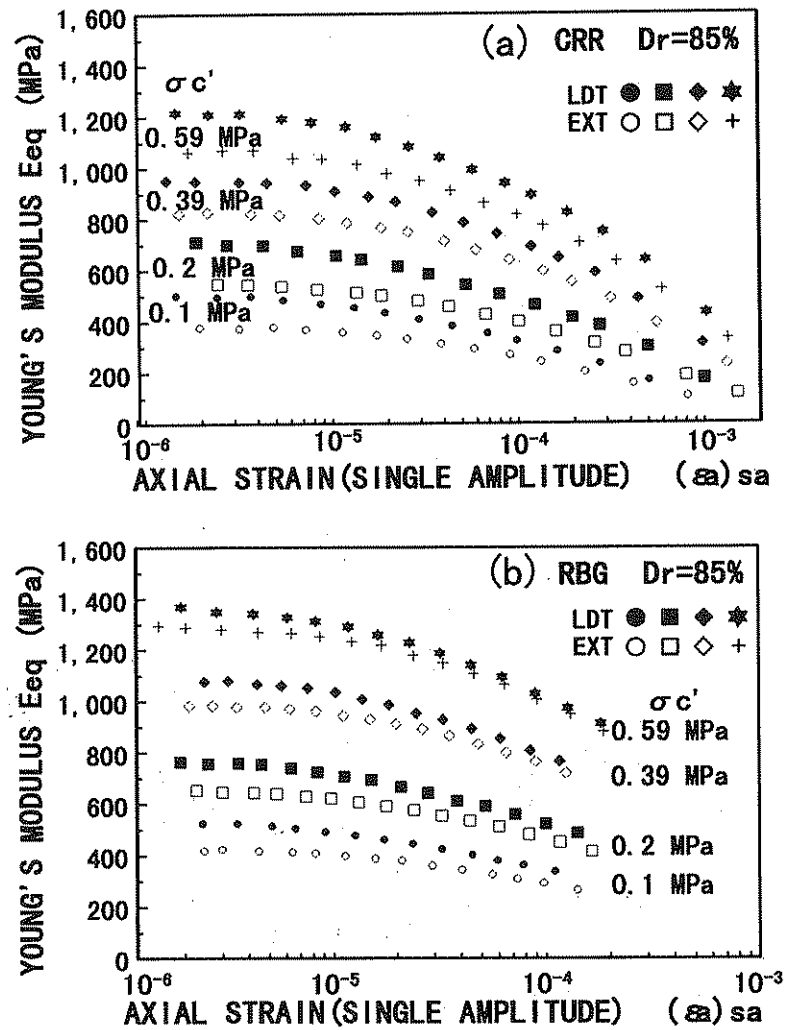


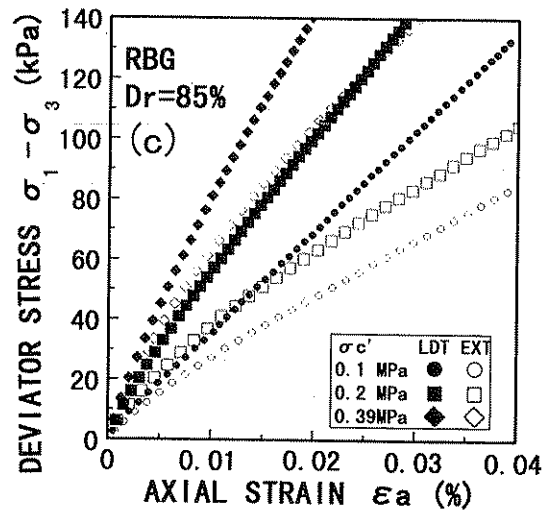
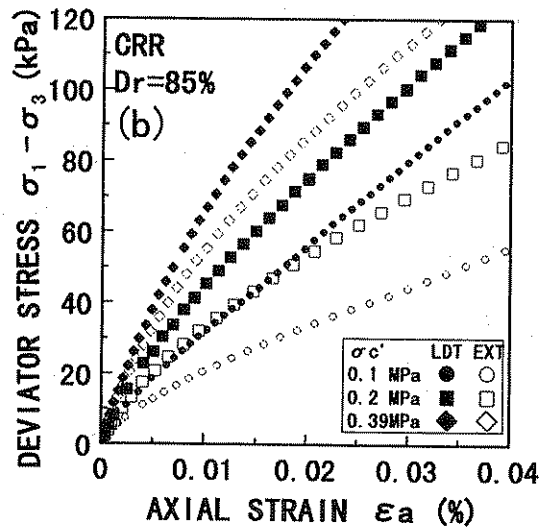
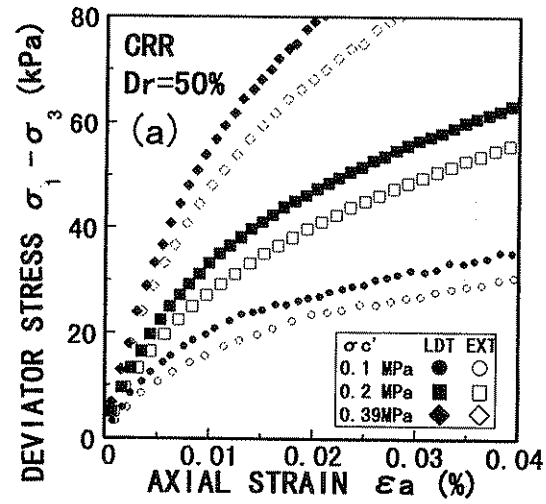
Figure 2 Illustration of process of cyclic loading test



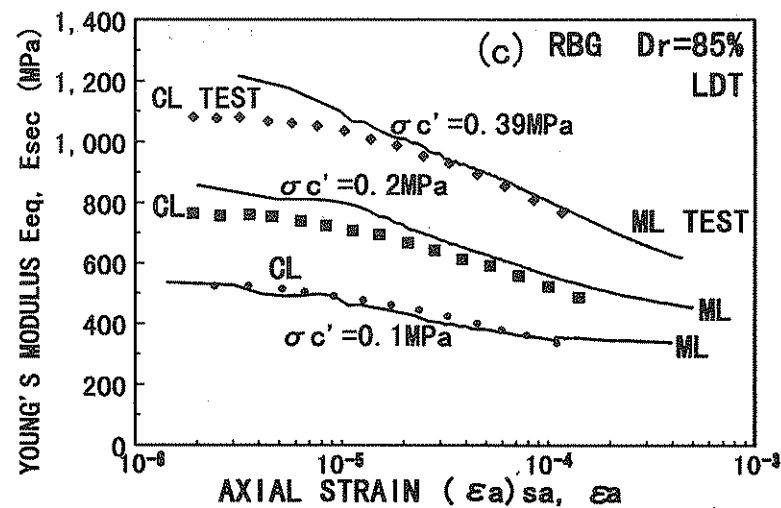
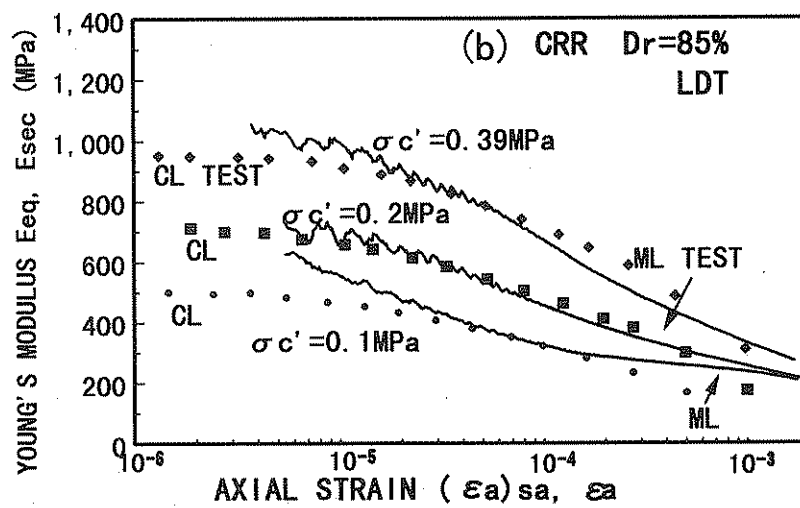
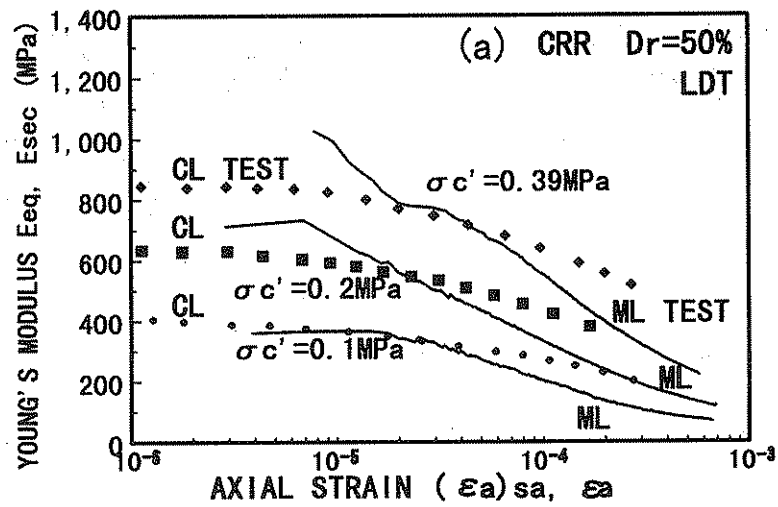
Figures 3 Definitions of Young's moduli from (a) cyclic and (b) monotonic loading



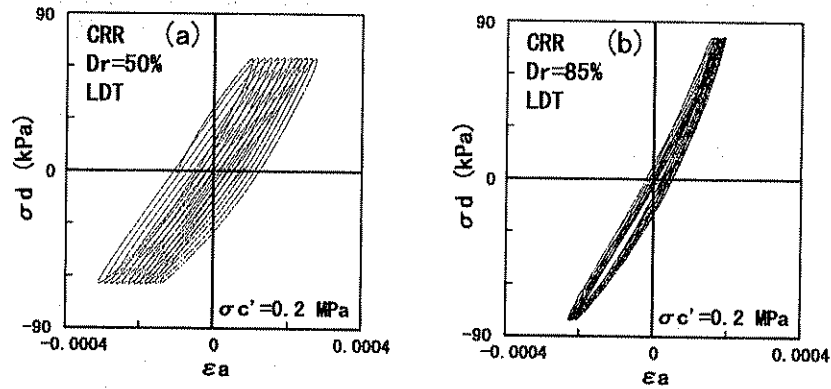
Figures 4 Comparisons of $E_{eq} \sim (\epsilon a)_{sa}$ measured locally and externally in cyclic loading triaxial tests; (a) CRR and (b) RBG



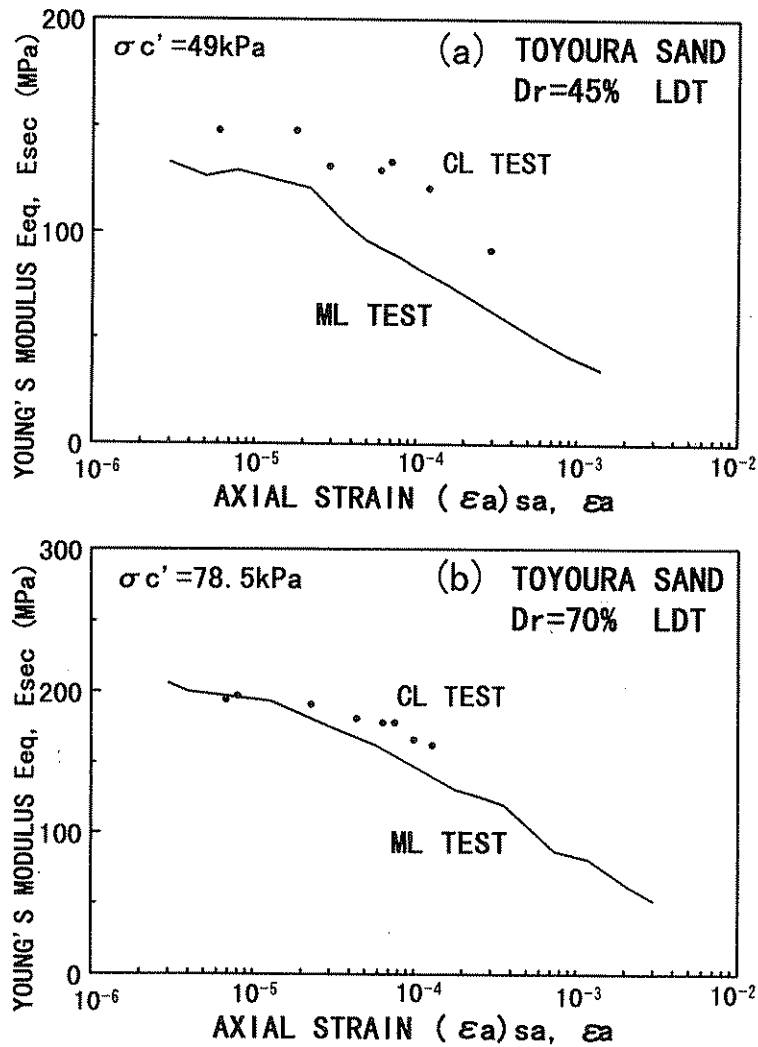
Figures 5 Comparisons of deviator stress $\sim \epsilon_a$ measured locally and externally in monotonic loading triaxial tests; (a) loose CRR and (b) dense CRR



Figures 6 Comparisons of $E_{eq} \sim (\epsilon_a)_{sa}$ from cyclic loading tests and $E_{sec} \sim \epsilon_a$ from monotonic loading tests; (a) loose CRR, (b) dense CRR, and (c) dense RBG



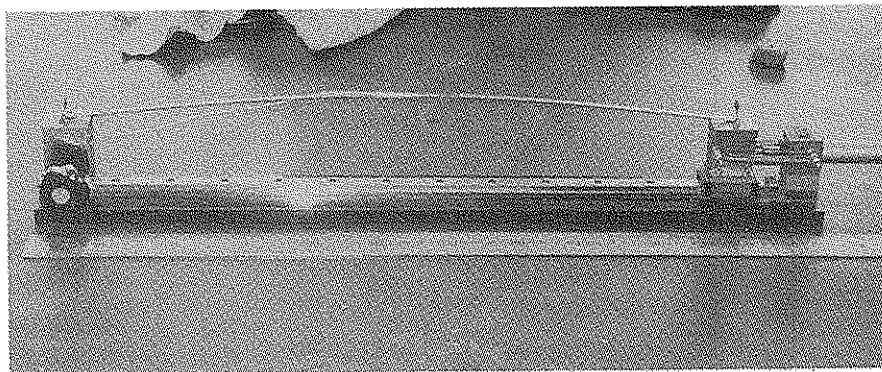
Figures 7 Hysteresis loops from cyclic loading tests at $(\epsilon_a)_{sa} = 2 \times 10^{-4}$;
(a) loose CRR, (b) dense CRR



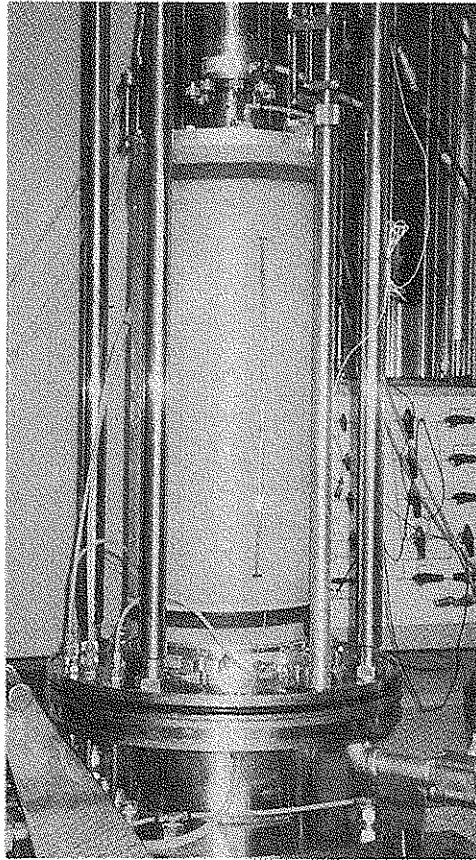
Figures 8 Comparisons of $E_{eq} \sim (\epsilon_a)_{sa}$ from cyclic loading tests and $E_{sec} \sim \epsilon_a$ from monotonic loading tests; (a) loose Toyoura sand and (b) dense Toyoura sand (Tatsuoka et al., 1994)



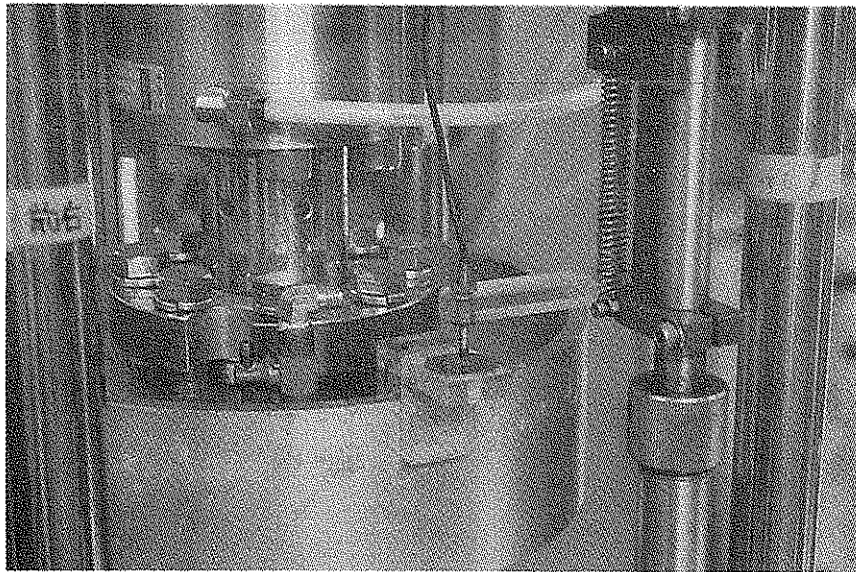
Photograph 1 Large-scale triaxial testing apparatus



Photograph 2 Local deformation transducer (LDT)



Photograph 3 LDT attached on the side of a specimen of coarse-grained materials



Photograph 4 Gap sensor and target attached on the top cap of a specimen